Chinese Chemical Letters 37 (2026) 111786

Contents lists available at ScienceDirect

Chinese Chemical Letters

journal homepage: www.elsevier.com/locate/cclet

Discovery of a novel cardiac myosin inhibitor for the treatment of hypertrophic cardiomyopathy

Anqi Shi[1], Jiahao Xiang[1], Qingyun Zhang, Minghui Tan, Wen Xiao, Yang Yang, Lin Zhao, Jian Liu, An Pan*, Junwei Wang*, Lihong Hu*

Jiangsu Key Laboratory for Functional Substance of Chinese Medicine, School of Pharmacy, Nanjing University of Chinese Medicine, Nanjing 210023, China

ARTICLE INFO

Article history:
Received 1 July 2025
Revised 3 September 2025
Accepted 4 September 2025
Available online 5 September 2025

Keywords:
Hypertrophic cardiomyopathy
Cardiac myosin inhibitor
Safety
Pharmacokinetic properties
Structural optimization

ABSTRACT

Inhibiting the contraction of cardiac myosin is an important strategy for treating hypertrophic cardiomyopathy (HCM). However, currently only MYK-461 has been approved for market, and its safety and pharmacokinetic (PK) properties still have deficiencies. Herein, we reported the discovery of a novel and potent cardiac myosin inhibitor Z5–11 through rational structural optimization of MYK-461. Compared with MYK-461, Z5–11 exhibited stronger inhibitory activity against myosin ATPase and could significantly inhibit myocardial cell contraction, as well as alleviate Ang II-induced cardiac hypertrophy. The cytotoxicity assessment on rat myocardial cells showed that Z5–11 exhibited better safety than MYK-461. The PK study revealed that Z5–11 had reasonable half-life time ($t_{1/2}=2.74$ h), and excellent oral bioavailability ($F=105.2$ %). More importantly, Z5–11 can effectively ameliorate transverse aortic constriction (TAC)-induced cardiac dysfunction and cardiac hypertrophy and remodeling in mice. These findings suggest that Z5–11 can be developed as a promising drug candidate for treating HCM.

© 2026 Published by Elsevier B.V. on behalf of Chinese Chemical Society and Institute of Materia Medica, Chinese Academy of Medical Sciences.

Hypertrophic cardiomyopathy (HCM) is a common hereditary cardiac disorder characterized by abnormal thickening of the left ventricular walls [1]. If not treated promptly, it can progress to heart failure (HF) [2,3]. According to statistical data, one in every 3200 individuals is affected by HCM, and approximately two-thirds of HCM patients progress to obstructive HCM (oHCM) [4,5]. In this pathological condition, asymmetric septal hypertrophy of the ventricular septum impedes the outflow of blood from the left ventricle, thereby leading to an elevated pressure gradient in the left ventricular outflow tract (LVOT) [6,7]. To combat cardiac hypertrophy, a variety of therapeutic options have been investigated, such as angiotensin converting enzyme inhibitors (ACEI), angiotensin receptor blockers (ARB), angiotensin receptor neprilysin inhibitors (ARNI), β-blockers, mineralocorticoid receptor antagonists (MRA), sodium-dependent glucose transporters 2 inhibitors (SGLT2i), and soluble guanylate cyclase (sGC) stimulators [8–10]. However, these approaches can alleviate symptoms and enhance quality of life, but are incapable of providing a complete cure [11,12]. Researchers have found that cardiac myosin mutations-induced hypercontractility leads to activation of signaling pathways that cause hypertrophy of the heart, fibrosis, and myofilament disarray [13]. Therefore, direct inhibition of cardiac sarcomere contractility may be a viable approach to treat HCM.

Mavacamten (MYK-461) was the first small molecule allosteric inhibitor of cardiac myosin approved by the U.S. Food and Drug Administration (FDA) for treating oHCM in 2022 [14,15]. It modulates cardiac contractility by selectively targeting the myosin-S1 motor and interfering with multiple stages of the myosin chemomechanical cycle to inhibit sarcomere force production [16,17]. In addition to its inhibitory effect on cardiac myosin ATPase activity, MYK-461 further ameliorates hypercontractility and LVOT obstruction by reducing actin-myosin cross-bridge formation and attenuating sarcomeric hyperactivation [18]. This dual mechanism not only decreases excessive systolic force generation but also improves diastolic relaxation, thereby mitigating the pathological hemodynamic consequences of HCM. Despite demonstrated clinical benefit of MYK-461 in oHCM patients, serious side effects were also observed [19]. For example, the human half-life ($t_{1/2}$) of MYK-461 is quite long, approximately ranging from 7 days to 9 days [20,21]. Therefore, it takes about 6 weeks for the drug concentration to reach a stable level, which may lead to various safety issues caused by drug accumulation [22,23]. Additionally, MYK-461 shows CYP3A4 and CYP2B6 induction in human hepatocytes, suggesting that it may cause drug-drug interactions (DDIs) due to the different clearance mechanisms of concomitant medications [24–26]. There-

* Corresponding authors.
E-mail addresses: panan@njucm.edu.cn (A. Pan), jwwang@njucm.edu.cn (J. Wang), lhhu@njucm.edu.cn (L. Hu).
[1] These authors contributed equally to this work.

https://doi.org/10.1016/j.cclet.2025.111786
1001-8417/© 2026 Published by Elsevier B.V. on behalf of Chinese Chemical Society and Institute of Materia Medica, Chinese Academy of Medical Sciences.

fore, the administration of MYK-461 requires strict adherence to a complex dose escalation regimen and thorough risk assessment [27].

To address the issues with MYK-461, MyoKardia company designed and synthesized a series of bicyclic pyrimidinedione compounds by the intramolecular cyclization of MYK-461, and developed the second therapeutic candidate MYK-224, which exhibited shorter half-life and reduced risk of CYP induction [28,29]. The phase I clinical trial of MYK-224 in healthy volunteers has been completed, and further clinical trials are currently underway [30]. These findings suggest that cyclization modification is a feasible strategy for improving the PK properties of MYK-461. Furthermore, aficamten (CK-274), a novel cardiac myosin inhibitor developed by cytokinetics for the treatment of symptomatic oHCM, is also currently in phase III clinical trials [31,32]. Compared with its predecessor MYK-461, CK-274 has more stable PK properties and a lower potential risk of drug interactions. Overall, although MYK-461 has been approved for the treatment of HCM, its safety and efficacy still need to be improved. Therefore, the discovery of novel cardiac myosin inhibitor with improved PK properties and safety is of great significance (Fig. S1 in Supporting information).

In this study, a series of novel cardiac myosin inhibitors were designed and synthesized by ingeniously cyclizing the ethylbenzene part of MYK-461 to form a tetrahydronaphthalene ring. Through systematic biological activity and pharmacokinetic (PK) properties evaluations, were discovered a novel and potent cardiac myosin inhibitor Z5–11, which effectively alleviated cardiac hypertrophy and exhibited high oral bioavailability and a reasonable half-life (Fig. 1A).

To facilitate the rational design, we first predicted the binding mode of MYK-461 to cardiac myosin by molecular docking. Since the crystal structure of MYK-461 to cardiac myosin has not been reported, the crystal structure of blebbistatin bound to an analogous myosin II from *Dictyostelium discoideum* (PDB: 1YV3) was used for the docking studies [33,34]. As shown in Figs. 1B and C, MYK-461 showed excellent shape complementarity with the binding pocket of myosin II, and the pyrimidone scaffold formed three key hydrogen bonds with Leu263, Lys265 and Ser266. The isopropyl and benzylamine groups were located in hydrophobic cavity A and B, respectively. The volume of cavity B was larger, suggesting that structural modification around the benzylamine group was feasible, and increasing the volume of the substituents would better occupy the hydrophobic cavity. Based on the above analysis and in combination with the patent protection scope of MYK-461, we designed a series of new cardiac myosin inhibitors by cyclizing the ethylbenzene of MYK-461 to a tetrahydronaphthalene ring. To verify rationality of our design, the docking study of designed compound Z5–8 with myosin was performed. As shown in Figs. 1D and E, the pyrimidone scaffold of Z5–8 could also form three key hydrogen bonds with Leu263, Lys265 and Ser266, and the spatial configuration of the tetrahydronaphthalene ring was basically consistent with the ethylbenzene of MYK-461.

Encouraged by this promising result, a series of indolone derivatives bearing isoxazole hydrophobic cap were designed and synthesized by varying the R^1, R^2 and R^3 substituents. To assess the potential cardiac myosin inhibitory activity of these designed compounds, we developed an *in vitro* assay for detecting the myosin ATPase inhibitory activity based on the principle that MYK-461 binds to the myosin-S1 motor domain and inhibits its ATPase activity. The results were shown in Tables S1 and S2 (Supporting information) and the structure-activity relationships (SARs) were detailly summarized.

Based on the SARs study, compounds Z5–3 and Z5–11 with higher myosin ATPase inhibition rate were chosen for further determination of the half maximal inhibitory concentration (IC_{50}) value, and MYK-461 and CK-274 were used as positive controls. As shown in Figs. 2A–D, Z5–11 displayed excellent myosin ATPase inhibitory activity with the IC_{50} values of 0.66 μmol/L, which was much stronger than that of MYK-461 (IC_{50}: 1.13 μmol/L) and CK-274 (IC_{50}: 1.43 μmol/L), respectively. Besides, Z5–3 showed similar myosin ATPase inhibitory activity (IC_{50}: 1.12 μmol/L) to MYK-461. Furthermore, the binding affinity of Z5–11 to cardiac myosin was detected by surface plasmon resonance analysis. The result revealed that Z5–11 exhibited stronger binding affinity than MYK-461 with the dissociation constant (K_d) values of 1.02 and 4.94 μmol/L, respectively (Figs. 2E and F). Taken together, the above results suggest that Z5–11 is a potent myosin ATPase inhibitor.

To better understand the binding mode between Z5–11 and myosin, we conducted a molecular docking study. As shown in Fig. 2G, Z5–11 exhibited excellent complementarity in the binding pocket of myosin II (PDB: 1YV3). In detail, the pyrimidone scaffold formed two key hydrogen bonds with Leu263 and Lys265. The oxygen atom on the pyran ring form a hydrogen bond with Lys423. The tetrahydronaphthalene ring occupied the hydrophobic cavity. To understand the binding stability of Z5–11 to myosin II, a molecular dynamic (MD) simulation at 100 ns was carried out using the Desmond Module of Schrödinger Maestro software (Fig. 2H). The protein backbone root-mean-square derivation (RMSD) plot analysis of myosin II-Z5–11 complex revealed that a stable RMSD of 3.2 Å was achieved after 50 ns of simulation. Furthermore, the binding free energy was calculated using the molecular mechanics generalized Born surface area (MM-GBSA) method. As depicted in Fig. 2I, the total binding free energy between Z5–11 and myosin II was −124.70 kcal/mol, and the higher van der Waals energy (−67.88 kcal/mol) and nonpolar solvation energy (−56.06 kcal/mol) made major contributions to the binding free energy.

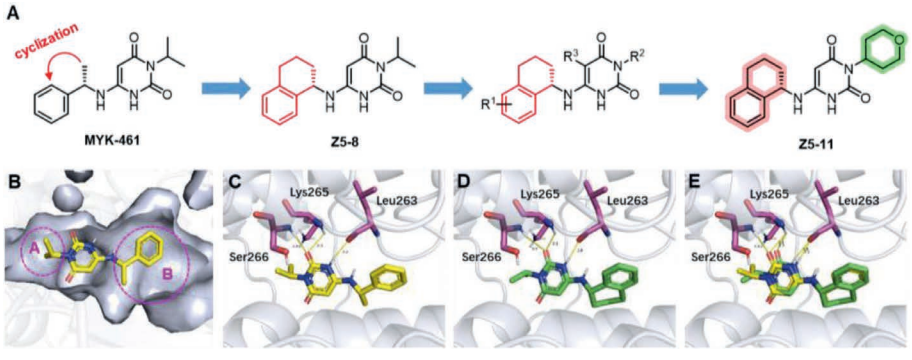


Fig. 1. Structure-based design of novel cardiac myosin inhibitors. (A) The overall design concept based MYK-461. (B, C) The predicted binding mode of MYK-461 with myosin II (PDB ID: 1YV3). (D) The predicted binding mode of Z5–8 with myosin II (PDB ID: 1YV3). (E) Comparison of the binding mode of MYK-461 and Z5–8 in the binding pocket of myosin II (PDB ID: 1YV3).

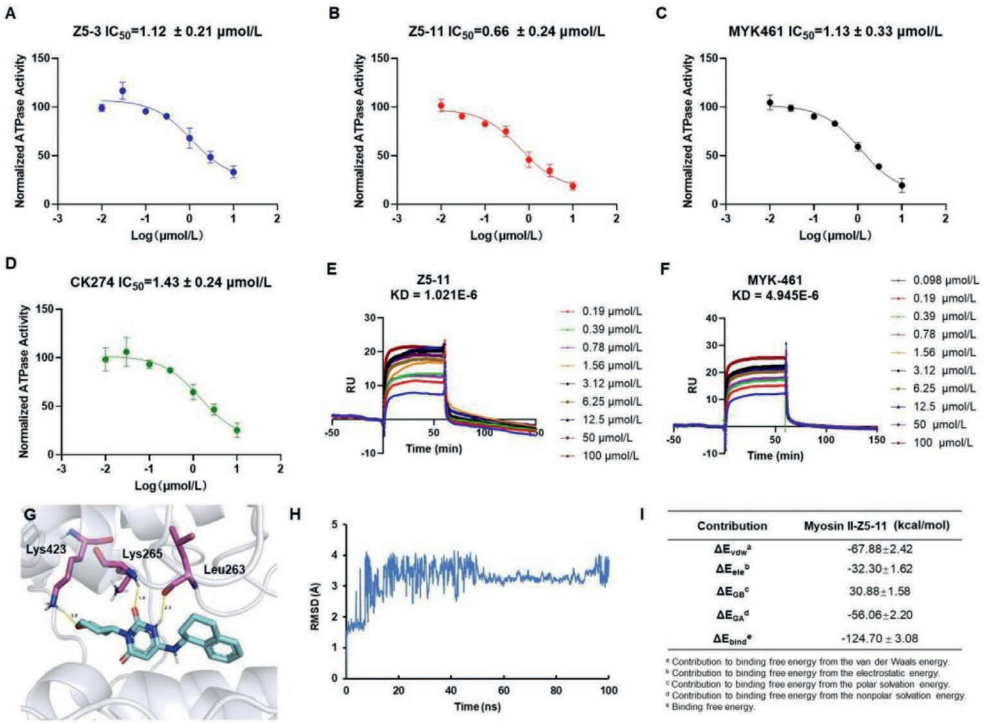


Fig. 2. Z5–11 and Z5–3 show potent myosin ATPase inhibitory activity. The IC_{50} values of myosin ATPase inhibitory activity for Z5–3 (A), Z5–11 (B), MYK-461 (C), and CK274 (D). IC_{50} values were presented as mean ± SD ($n = 3$). (E, F) The binding affinity of Z5–11 or MYK-461 to the cardiac myosin confirmed by surface plasmon resonance. (G) Predicted binding mode of Z5–11 to an analogous myosin II (PDB: 1YV3). (H) The protein backbone RMSD plot of myosin II-Z5–11 complex. (I) Binding free energy of myosin II-Z5–11 complex and its contributions.

Encouraged by the potent myosin ATPase inhibitory activity, the effects of Z5–11 and Z5–3 on the contraction of myocardial cells and myocardial hypertrophy were evaluated. We isolated neonatal rat cardiomyocytes (NRCMs) and placed cell suspension in a perfusion chamber integrated with the microscope stage, followed by synchronized application of electric field stimulation and a certain concentration of drug intervention. The contraction amplitude and other contraction indicators of myocardial cells before and after drug administration were detected using the IonOptix measurement system to calculate the inhibition rate of compounds on myocardial cell contraction. The results illustrated the inhibitory effects of Z5–11 and Z5–3 on the contractility of NRCMs were summarized in Table S3 (Supporting information). A significant reduction in myocyte contractility as measured by myocyte length was observed upon treatment with these two compounds relative to a predose measurement. More exactly, Z5–11 demonstrated dose-dependent inhibitory effect on myocardial cell contraction, achieving an inhibition rate of 80.7 % at a concentration of 1 μmol/L, significantly surpassing that of MYK-461 (58.7 %).

To more directly observe the ameliorative effects of Z5–11 and Z5–3 on cardiac hypertrophy *in vitro*, we isolated NRCMs and investigated the effects of these compounds (0.1, 1, 10 μmol/L) on NRCMs under Ang II stimulation (Fig. 3A). As expected, hypertrophic markers (*Nppa, Nppb*) and fibrosis markers (*Col1a1, Acta2*) were significantly down-regulated after Z5–11 and Z5–3 treatment compared to Ang II group (Figs. 3B–E). Moreover, both Z5–11 and Z5–3 (1 μmol/L) treatments markedly attenuated Ang II-induced cardiomyocyte hypertrophy, as demonstrated by cytoskeletal analysis of myocardial cells (Fig. 3F). These results strongly suggest that Z5–11 and Z5–3 can alleviate Ang II-induced cardiac hypertrophy *in vitro*.

Prior to the *in vivo* efficacy study, we evaluated the *in vitro* safety of Z5–11, Z5–3 and MYK-461. Rat myocardial cells H9C2 were cultured and treated with varying concentrations of these compounds, followed by cytotoxicity assessment using the cell counting kit-8 (CCK-8) assay. The results demonstrated that H9C2 cell viability was markedly reduced at the concentration of 100 μmol/L after Z5–3 and MYK-461 treatments, whereas Z5–11 showed no significant cytotoxicity even at the concentration as high as 100 μmol/L (Fig. S2 in Supporting information). These results indicated that the safety of Z5–11 has been significantly improved compared to MYK-461.

To investigate whether the *in vivo* metabolisms of Z5–11 and Z5–3 have been improved, we evaluated the PK parameters of these two compounds in Sprague Dawley rats through intravenous injection (i.v., 2.5 mg/kg) and oral administration (p.o., 5 mg/kg). As depicted in Table 1, the half-lives of Z5–11 and Z5–3 were 2.74 h and 4.25 h, respectively, which were significantly shorter compared to MYK-461 ($t_{1/2} = 8.2$ h) [20]. Among which, Z5–11 showed the optimal PK properties with high plasma exposure, reasonable half-life time ($t_{1/2} = 2.74$ h), and high oral bioavailability ($F = 105.2$ %). Overall consideration of the myosin inhibitory activity, safety and PK properties, Z5–11 was selected for further biological evaluation *in vivo*.

To investigate the cardioprotective effects of Z5–11 on mice with cardiac hypertrophy, we created mouse models through transverse aortic constriction (TAC) and administered Z5–11 for 4 weeks (Fig. 4A). To comprehensively evaluate cardiac function and myocardial remodeling in each group, we performed B-mode echocardiography to assess global cardiac structure and M-mode imaging to measure left ventricular wall thickness at end-systole and end-diastole (Fig. 4B).

Echocardiographic assessment demonstrated that Z5–11-treated mice exhibited attenuated cardiac dilation and improved functional preservation after TAC, as evidenced by key parameters including: left ventricular end-diastolic anterior wall thickness (LVAWd), left ventricular end-systolic anterior wall thickness (LVAWs), left ventricular posterior wall diameter in diastole (LVPWd), left ventric-

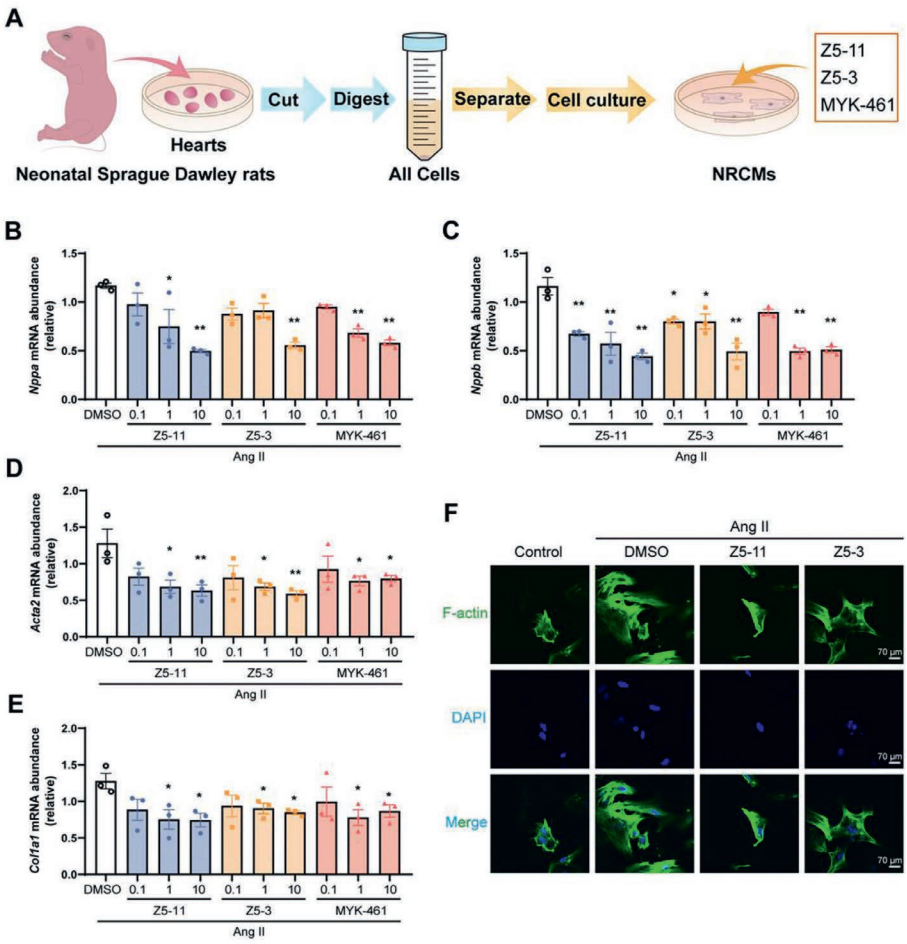


Fig. 3. Z5–11 and Z5–3 effectively inhibit myocardial hypertrophy. (A) Schematic overview of the experimental design. NRCMs were isolated from 1- to 3-day-old Sprague Dawley rats and cultured at 37 °C in a humidified incubator with 5 % CO_2 atmosphere. All cells were stimulated with 1 μmol/L Ang II and treated with different compounds. (B, C) Reverse transcription quantitative polymerase chain reaction (RT-qPCR) detection for hypertrophic biomarkers *Nppa* (B) and *Nppb* (C). $n = 3$ samples per group. (D, E) Fibrosis genes *Acta2* (D) and *Col1a1* (E) in the indicated groups determined by RT-qPCR. $n = 3$ samples per group. All normalized to *18 s* rRNA. (F) NRCMs morphology stained by F-actin (green). The nuclei were stained with 4′,6-diamidino-2-phenylindole dihydrochloride (DAPI) (blue). Scale bar: 70 μm. Cells were treated as in (A). Values represent mean ± SEM. Statistical differences were determined by one-way ANOVA. $^{*}P < 0.05$, $^{**}P < 0.01$ *vs.* DMSO group.

Table 1
PK study of Z5–11 and Z5–3 in Sprague Dawley rats.[a]

Parameters	Z5–11		Z5–3	
	p.o. (5 mg/kg)	i.v. (2.5 mg/kg)	p.o. (5 mg/kg)	i.v. (2.5 mg/kg)
$T_{1/2}$ (h)	2.74	3.65	4.25	0.78
T_{max}	0.25	–	0.33	–
T_{last} (h)	24	18.67	24	5.33
C_{max} (ng/mL)	1193.7	1349.87	1253.97	3327.30
C_{last} (ng/mL)	5.38	38.36	15.15	19.43
AUC_{last} (h ng mL^{-1})	6564.29	3111.16	3367.22	2764.97
AUC_{INF_obs} (h ng mL^{-1})	6570.50	3303.29	3460.41	2785.53
V_{Z_obs} (mL/kg)	–	4122.35	–	1020.97
$CL_{_obs}$ (mL h^{-1} kg^{-1})	–	775.58	–	919.30
F	105.21 %	–	60.89 %	–

[a] Values are the average of three runs. $T_{1/2}$, terminal half-life; C_{max}, maximum observed concentration occurring at T_{max}; T_{max}, time of C_{max}; C_{last}, last measurable positive concentration; T_{last}, time of C_{last}; AUC_{last}, area under the concentration *vs.* time curve from the first observed to last measurable concentration; AUC_{INF_obs}, area under the concentration-time curve from time 0 to infinity; V_{Z_obs}, volume of distribution; $CL_{_obs}$, clearance; *F*, oral bioavailability. –Not applicable.

ular posterior wall diameter in systole (LVPWs), ejection fraction (EF), left ventricular mass (LV mass), and fractional shortening (FS) (Figs. 4C–I).

Furthermore, morphological analysis revealed that TAC surgery induced significant cardiac hypertrophy, which was markedly attenuated by Z5–11 and MYK-461 treatment (Figs. 4J–L). In detail, WGA staining confirmed cardiomyocyte hypertrophy, and Masson staining detected fibrosis in TAC-treated mouse heart tissue (Fig. 4M). While Z5–11 and MYK-461 treatment effectively attenuated cardiac inflammation and fibrosis, as evidenced by histological staining (Fig. 4M). Additionally, Z5–11 and MYK-461 significantly suppressed TAC-induced expression of fetal cardiac genes (atrial natriuretic peptide (ANP), brain natriuretic peptide (BNP)) and fibrosis markers (Figs. 4N and O). Collectively, these results demonstrated that Z5–11 had a significant protective effect on TAC-induced cardiac hypertrophy and fibrosis. All experimental an-

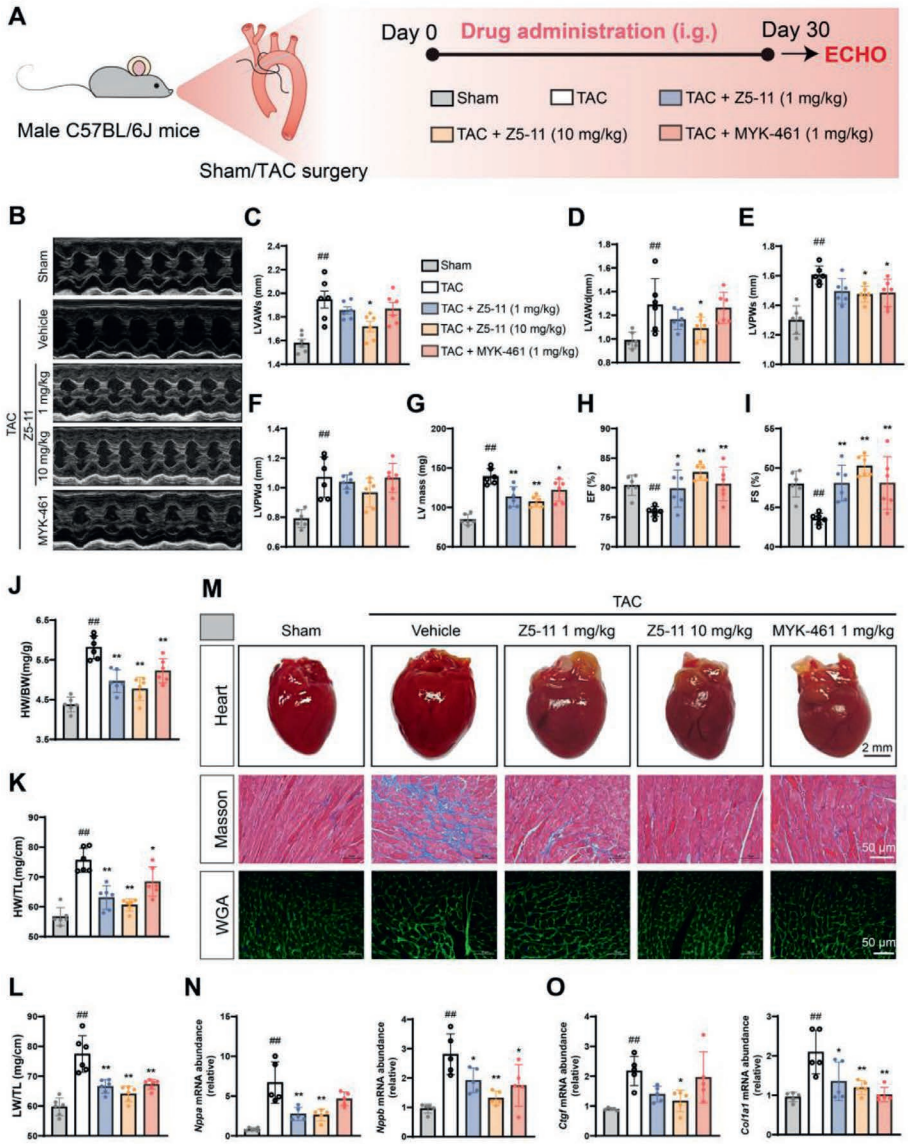


Fig. 4. Z5–11 ameliorates TAC-induced cardiac hypertrophy and remodeling in mice. (A) Schematic overview of the experimental design in the mice model. The mice were subjected to TAC and then treated with Z5–11 (intragastric administration (i.g.) 1 or 10 mg kg^{-1} d^{-1}) or MYK-461 (i.g. 1 mg kg^{-1} d^{-1}) for 30 days. (B–I) Representative M-mode images (B) and statistical analysis of LVAWs (C), LVAWd (D), LVPWs (E), LVPWd (F), LV Mass (G), EF% (H) and FS% (I). $n = 6$ samples per group. (J–L) The ratio of heart weight to body weight (HW/BW, J), heart weight to tibia length (HW/TL, K) and lung weight to tibia length (LW/TL, L). $n = 6$ samples per group. (M) Representative gross images of whole hearts (scale bar: 2 mm), cell boundaries demarcated with fluorescein isothiocyanate-wheat germ agglutinin and Masson's trichrome (scale bar: 50 μm). (N, O) RT-qPCR analysis of hypertrophic markers (*Nppa* and *Nppb,* N) and fibrosis genes (*Ctgf* and *Col1a1,* O). $n = 5$ samples per group. All normalized to *Actb*. Values represent mean ± SEM. Statistical differences were determined by one-way ANOVA. $^{\#}P < 0.05$, $^{\#\#}P < 0.01$ *vs.* sham group; $^{*}P < 0.05$, $^{**}P < 0.01$ *vs.* TAC group.

imal protocols were reviewed and approved by Nanjing University of Chinese Medicine Animal Ethics Committee (approval No. 202205A056), complying with Guidelines for the Care and Use of Laboratory Animals.

In summary, through rational structural optimization and systematic biological evaluation, we identified a novel and potent cardiac myosin inhibitor Z5–11. It not only displayed stronger myosin ATPase inhibitory activity, but also had a significant inhibitory effect on cardiac myocyte contraction, and can alleviate Ang II-induced cardiac hypertrophy. Notably, the safety and of PK parameters of Z5–11 were significantly improved compared to MYK-461. Moreover, Z5–11 can effectively ameliorate TAC-induced cardiac dysfunction and cardiac hypertrophy and remodeling in mice. These results strongly supported the potential of Z5–11 as a therapeutic approach for HCM.

Declaration of competing interest

The authors declare that they have no known competing financial interests or personal relationships that could have appeared to influence the work reported in this paper.

CRediT authorship contribution statement

Anqi Shi: Writing – original draft, Methodology, Investigation, Formal analysis, Data curation. **Jiahao Xiang:** Writing – original draft, Validation, Investigation, Data curation. **Qingyun Zhang:** Validation, Methodology, Data curation. **Minghui Tan:** Methodology, Investigation. **Wen Xiao:** Visualization, Validation. **Yang Yang:** Software, Formal analysis. **Lin Zhao:** Investigation, Data curation. **Jian Liu:** Visualization, Software. **An Pan:** Writing – original draft,

Validation, Project administration, Formal analysis. **Junwei Wang:** Writing – review & editing, Resources, Project administration, Funding acquisition, Conceptualization. **Lihong Hu:** Supervision, Project administration, Funding acquisition, Conceptualization.

Acknowledgments

This work was supported by the National Natural Science Foundation of China (Nos. 82173664, 82304803), Natural Science Foundation of Jiangsu Province (No. BK20230461), the Natural Science Foundation of Jiangsu Province for Outstanding Yong Scholars (No. BK20220109), the Innovation Projects of State Key Laboratory on Technologies for Chinese Medicine Pharmaceutical Process Control and Intelligent Manufacture (No. NZYSKL240209), the Major Basic Research Project of the Natural Science Foundation of the Jiangsu Higher Education Institutions (No. 22KJA350003).

Supplementary materials

Supplementary material associated with this article can be found, in the online version, at doi:10.1016/j.cclet.2025.111786.

References

[1] C.W. Tsao, A.W. Aday, Z.I. Almarzooq, et al., Circulation 145 (2022) e153–e639.
[2] G.G. Schiattarella, J.A. Hill, Circulation 131 (2015) 1435–1447.
[3] W.X. Wu, B.B. Wang, Y. Qin, et al., Chin. Chem. Lett. 36 (2025) 110584.
[4] B.J. Maron, E.J. Rowin, M.S. Maron, JACC Heart Fail. 6 (2018) 376–378.
[5] S.R. Ommen, S. Mital, M.A. Burke, et al., Circulation 142 (2020) e533–e557.
[6] Y.K. Tham, B.C. Bernardo, J.Y. Ooi, K.L. Weeks, J.R. McMullen, Arch. Toxicol. 89 (2015) 1401–1438.
[7] A. Jaiswal, V.Q. Nguyen, B.J. Carry, T.H. le Jemtel, J. Card. Fail. 22 (2016) 829–839.
[8] S.Y. Zhang, J. Geriatr. Cardiol. 22 (2025) 277–331.
[9] B. Bozkurt, Nat. Rev. Cardiol. 21 (2024) 545–555.
[10] H. Yuan, F. Zhang, H. Huang, et al., Chin. Chem. Lett. 36 (2025) 109965.
[11] G.A. Nichols, K. Reynolds, T.M. Kimes, A.G. Rosales, W.W. Chan, Am. J. Cardiol. 116 (2015) 1088–1092.
[12] H. Dokainish, K. Teo, J. Zhu, et al., Lancet Glob. Health. 5 (2017) e665–e672.
[13] O. Tsukamoto, Int. J. Mol. Sci. 21 (2020) 226–238.
[14] MyoKardia, a wholly owned subsidiary of Bristol Myers Squibb, https://www.accessdata.fda.gov/drugsatfda_docs/label/2022/214998s000lbl.pdf, 2022.
[15] E. Braunwald, S. Saberi, T.P. Abraham, P.M. Elliott, I. Olivotto, Eur. Heart. J. 44 (2023) 4622–4633.
[16] R.F. Kawas, R.L. Anderson, S.R.B. Ingle, et al., J. Biol. Chem. 292 (2017) 16571–16577.
[17] W. Ma, C.L. Del Rio, L. Qi, et al., Proc. Natl. Acad. Sci. U. S. A. 121 (2024) e2314914121.
[18] N. Zatorski, E.A. Sobie, A. Schlessinger, Trends. Pharmacol. Sci. 44 (2023) 318–319.
[19] I. Olivotto, A. Oreziak, R. Barriales-Villa, et al., Lancet 396 (2020) 759–769.
[20] E.M. Green, H. Wakimoto, R.L. Anderson, et al., Science 351 (2016) 617–621.
[21] S.J. Keam, Drugs 82 (2022) 1127–1135.
[22] M.P. Grillo, J.C.L. Erve, R. Dick, et al., Xenobiotica 49 (2019) 718–733.
[23] Y. Xu, L. Wang, L. Yang, et al., Chin. Chem. Lett. 36 (2025) 110958.
[24] X. Wu, N. Chen, P. Hsu, et al., Clin. Transl. Sci. 17 (2024) e13877.
[25] G. Kayki-Mutlu, Z.S. Aksoyalp, L. Wojnowski, M.C. Michel, Naunyn Schmiedebergs Arch. Pharmacol. 396 (2023) 1619–1632.
[26] A. Humayra, C.S. Joseph, K. Mohsin, A.S. Rizwan, A. Majed, M. Nurunnabi, Chin. Chem. Lett. 33 (2022) 2773–2782.
[27] F.I. Malik, L.A. Robertson, D.R. Armas, et al., JACC Basic Transl. Sci. 7 (2022) 763–775.
[28] S.J. Lehman, C. Crocini, L.A. Leinwand, Nat. Rev. Cardiol. 19 (2022) 353–363.
[29] MyoKardia Programs MyoKardia, https://myokardia.com/programs, 2020 (accessed on 22 August 2020).
[30] AdisInsight. A phase 1 randomized, placebo-controlled, single and multiple-ascending dose study of myk-224 in healthy volunteers—AdisInsight. https://adisinsight.springer.com/trials/700301316 (accessed on 1 September 2020).
[31] M.S. Maron, A. Masri, M.E. Nassif, et al., N. Engl. J. Med. 390 (2024) 1849–1861.
[32] C. Chuang, S. Collibee, L. Ashcraft, et al., J. Med. Chem. 64 (2021) 14142–14152.
[33] J.S. Allingham, R. Smith, I. Rayment, Nat. Struct. Mol. Biol. 12 (2005) 378–379.
[34] J.J. Frye, V.A. Klenchin, C.R. BagShaw, I. Rayment, Biochemistry 49 (2010) 4897–4907.